JOURNAL OF SOLID STATE CHEMISTRY **121,** 138–142 (1996)
ARTICLE NO. 0020

Magnetic and Electric Properties of Bi(La)Sr(Ca)Mn_2O_6

Zeng Zuotao and Ren Yufang

Laboratory of Rare Earth Chemistry and Physics, Changchun Institute of Applied Chemistry, Chinese Academy of Sciences, Changchun 130022, P.R. China

Received May 24, 1995; in revised form August 29, 1995; accepted August 30, 1995

$Bi_{1-x}La_xSrMn_2O_6$ and $BiSr_{1-x}Ca_xMn_2O_6$ are prepared by solid state reaction. They are *n*-type semiconductors with ferromagnetism at room temperture. When Bi is substituted partly by rare earth, a negative magnetoresistance effect is observed in the pellet of $Bi_{1-x}La_xSrMn_2O_6$. There are semiconductor–metal transitions at 820 K in $BiSrMn_2O_6$. The transitions are attributed to the magnetic transition at high temperature. The substitution of Ca for Sr makes the transition temperature increase. However, when Bi is partly substituted by La, the solid solution does not change into metal.

INTRODUCTION

Some oxides of manganese such as $LaSr_3Mn_2O_8$ and $LaSrMnO_4$ are ferromagnetic when the valence of Mn is between +3 and +4 (1, 2). They are also semiconductors. The electric and magnetic properties of these manganates have been investigated extensively (3–7). Mn–O nets play a key role in charge transport. The itinerant electron ferromagnetism of these compounds is also attributed to Mn–O nets. Mn^{4+}–O–Mn^{3+} exchange coupling makes the compound become ferromagnetic. Recently, a very big magnetoresistance effect was observed in some manganate files such as $La_{1-x}Ba_xMnO_z$ and $La_{1-x}Ba_xMnO_z$ (8–13). They are perovskite-type structure with ferromagnetic ordering in the *a*–*b* planes. The ferromagnetically ordered Mn–O layers of the *a*–*b* planes are separated by a nonmagnetic La–O layer. This case is similar to that of metallic multilayers with a giant magnetoresistance effect. Therefore, it is interesting to investigate the magnetoresistance of manganate. A thousandfold resistivity change of these materials in magnetic field has been found. They are useful in many areas. In this paper, we report a new material, $Bi_{1-x}La_xSrMn_2O_6$, with a negative magnetoresistance in bulk.

We once investigated the electric properties of $BiSrMn_2O_6$ (14). Semiconductor–metal transition was observed around 820 K in the compound, and there is a change of activation energy around 490 K. However, what causes this change is not given in that paper. Now, we investigate the magnetic properties of this compound. There also are two transition points around 490 and 820 K in the plot of $1/X_M$–T. Therefore, it is considered that there are some relations between the change of electric property and magnetic properties, and the reason is explained here. The effect of substituting Ca for Sr and substituting La for Bi is also investigated.

EXPERIMENTAL

Samples were synthesized by a solid state reaction technique. Analytical reagents $SrCO_3$, $CaCO_3$, Bi_2O_3, Mn_2O_3, and 99.99% La_2O_3 were used as starting materials. The starting materials in stoichiometric proportion were mixed, ground, and sintered at 800°C for 24 hr. The resulting powders were reground, pressed, and sintered at 850°C for 24 h and cooled to room temperature in the furnace.

Resistivity was measured by a standard four-probe method on pressed, sintered pellets in the temperature range 300–1100 K.

A Shimadzu MB-II magnetic balance was used to measure susceptibility in the temperature range 300–1100 K.

Powder X-ray diffraction was carried on a Rigaku C/max-IIB X-ray diffractometer. A standard silicon powder sample was used to calibrate the experimental data.

The valence of Mn was determinated by chemical analysis (14).

TGA and DTA were carried out in a Rigaku Thermoflex thermal analysis system in air. The heating rate was 10°C/min.

RESULTS AND DISCUSSION

$BiSr_{1-x}Ca_xMn_2O_6$ are tetragonal. The unit cell parameters of these compounds are shown in Fig. 1. The unit cell parameters of $BiSr_{1-x}Ca_xMn_2O_6$ decrease as the contents of Ca increase. The radius of Ca^{2+} (0.100 nm) is smaller than that of Sr^{2+} (0.118 nm) (15). Therefore, the unit cell parameters of $BiSr_{1-x}Ca_xMn_2O_6$ decrease when Sr is substituted by Ca. Impurity phases appear for $x > 0.75$. We can not synthesize $BiCaMn_2O_6$. This may be the reason that the radius of Ca (0.100 m) is too small for the structure.

0022-4596/96 $12.00

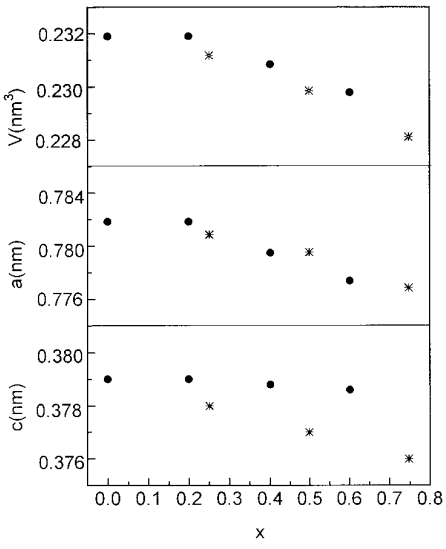

FIG. 1. Unit cell parameters versus x for (*) $BiSr_{1-x}Ca_xMn_2O_6$ and (●) $Bi_{1-x}La_xSrMn_2O_6$.

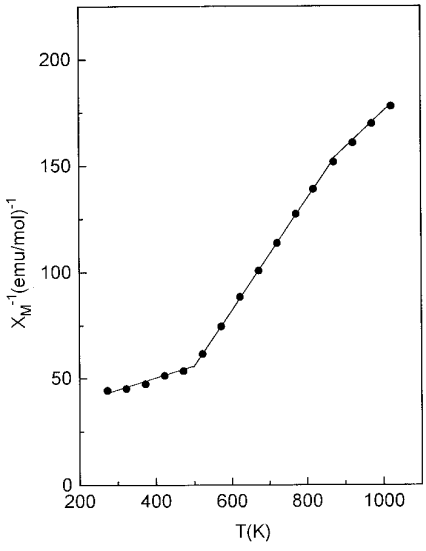

FIG. 2. Inverse susceptibility–temperature plot for $BiSrMn_2O_6$.

When Ca^{2+} ion concentration increases, the stability of the structure is lowered and it becomes unstable at $x = 0.75$.

Bi can also be substituted by La for $x \leq 0.6$ in $Bi_{1-x}La_xSrMn_2O_6$. The solid solution is still tetragonal. Its c axis scarcely changes. However, the a value decreases when Bi is substituted by La. The ionic radius of Bi^{3+} (0.103 nm) is nearly equal to that of La^{3+} (0.1032 nm) (15). Nevertheless, the size of Bi^{3+} depends on the degree of the $6s^2$ lone-pair character. When Bi^{3+} is forced into high symmetry, the size of Bi^{3+} is smaller than that of La^{3+}, but when lone-pair character is dominant, the Bi^{3+} compound is distorted and the volume of the Bi^{3+} compound may be larger than that of the La^{3+} compound. For example, the volume of $LaTaO_3$ is smaller than that of $BiTaO_3$, where the long-pair character of Bi^{3+} is dominant (16). The long-pair character of Bi^{3+} also makes the structure distort from monoclinic $LaTaO_3$ to triclinic $BiTaO_3$. In $Bi_{1-x}La_xSrMn_2O_6$, the lone-pair character of Bi^{3+} may be dominant. Therefore, the volume of $Bi_{1-x}La_xSrMn_2O_6$ decreases with increasing contents of La^{3+}. When Bi is substituted by La, the distortion which is caused by the lone-pair character of Bi^{3+} decreases. Therefore, only the a axis decreases and the b axis does not change when Bi is substituted by La.

There are two transition points in the plot of $1/X_M$–T for $BiSrMn_2O_6$, which is shown in Fig. 2. In an early experiment, it was found that Mn^{4+}–O–Mn^{4+} exchange coupling is antiferromagnetic while that of Mn^{4+}–O–Mn^{3+} is strongly ferromagnetic (2). In this compound, the valence of Mn is between +3 and +4. It is also ferromagnetic below 490 K. The long-range ferromagnetic order vanishes above 490 K. The compound shows Curi–Weiss behavior above 490 K, with $\theta = 280$ K between 490 and 820 K. There is another transition at 820 K. θ is about 70 K for the compound above 820 K.

The electronic configuration of Mn^{4+} is $t_{2g}^3e_g^0$. However, there are two types of electronic configuration of Mn^{3+}. It is $t_{2g}^3e_g^1$ at high-spin state and $t_{2g}^4e_g^0$ at low-spin. The effective magneton number is (17)

$$\mu_{\text{eff}} = 2[S(S+1)]^{1/2}.$$

If Mn^{3+} is at low-spin state, S is 1 and the calculated μ_{eff} is $2.83\mu_B$. If Mn^{3+} is at high-spin state, S is 2 and the calculated μ_{eff} is $4.90\mu_B$. The experimental μ_{eff} is $4.9\mu_B$ (17). The μ_{eff} is $3.87\mu_B$ for Mn in $BiSrMn_2O_{6.02}$. For $BiSrMn_2O_{6.02}$, the oxidation state of Mn is $3.52\mu_B$. The formal ratio of Mn^{3+}/Mn^{4+} is approximately 1 : 1. If all of the Mn^{3+} is at high-spin state, μ_{eff} should be about $4.4\mu_B$. If all of the Mn^{3+} is at low-spin state, μ_{eff} should be about $3.35\mu_B$. However, μ_{eff} of $BiSrMn_2O_{6.02}$ is $3.93\mu_B$ between 490 and 820 K. Therefore, it may be assumed that some of the Mn ions are at low-spin state and some of Mn ions are at high-spin state in $BiSrMn_2O_{6.02}$. Above 820 K, μ_{eff} increases to $4.6\mu_B$. The value is near the μ_{eff} when the Mn ions are half Mn^{3+} and half Mn^{4+}. At high temperature, the low-spin state may be excited to high-spin state and cause the transition at 820 K.

The substitution of Ca for Sr makes resistivity decrease. The resistivities at room temperature are shown in Fig. 3. Figure 4 shows the plot of ln ρ vs $1/T$ for $BiSrMn_2O_6$ and $BiSr_{0.5}Ca_{0.5}Mn_2O_6$. There are also two transition points in the plot of ln ρ vs $1/T$ for $BiSrMn_2O_6$. The values of two transition points, 490 and 820 K, are the same as that of

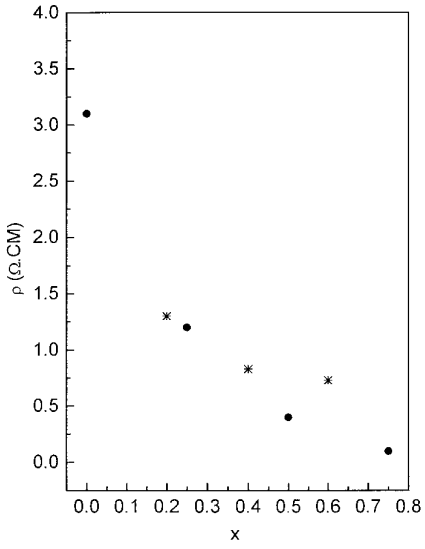

FIG. 3. Resistivities versus x for (●) $BiSr_{1-x}Ca_xMn_2O_{6+x}$ and (*) $Bi_{1-x}La_xSrMn_2O_6$.

the two points in the plot of $1/X_M$–T. There is not an obvious change of structure and oxygen contents near 490 and 820 K. Figure 5 shows the DTA and TG thermal analysis results. Therefore, there may be some relation between magnetic properties and electron transport.

Electrons transport through the Mn–O nets in this compound (7). The 3*d* electrons of Mn play a key role in the transport. They are also important to form the long-range ferromagnetic order. The band model may be also used to account for the ferromagnetism of this compound (17).

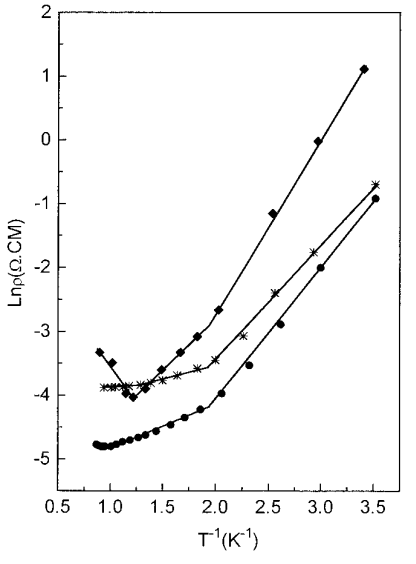

FIG. 4. Resistivities versus temperature for (◆) $BiSrMn_2O_6$, (●) $BiSr_{0.5}Ca_{0.5}Mn_2O_6$, and (*) $Bi_{0.5}La_{0.5}SrMn_2O_6$.

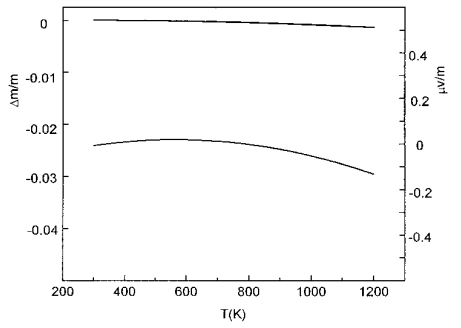

FIG. 5. Plot of DTA and TG thermal analysis for $BiSrMn_2O_6$.

According to this model, the 3*d* energy band may be separated into two sub-bands below Curie temperature and cause ferromagnetic order. Above Curie temperature, the ferromagnetic order vanishes and the 3*d* energy band changes. This makes the activation energy change. Therefore, the activation energy changes when the spontaneous magnetization vanishes above Curie temperature.

The semiconductor–metal transition appears at 820 K. At the same temperature, a magnetic transition occurs, which may be caused by the excitation from $t_{2g}^4e_b^0$ to $t_{2g}^3e_g^1$. The excitation from low-spin to high-spin makes the energy band change and also makes the semiconductor change to metal. This is like the transition in $LaCoO_3$ (18).

Just like in $BiSrMn_2O_6$, there are also two transition points in the plot of ln ρ vs $1/T$ for $BiSr_{0.5}Ca_{0.5}Mn_2O_6$. The first point appears at 510 K, which is a little higher than the transition temperature of $BiSrMn_2O_6$. The activation energy is 0.18 eV below 500 K. It decreases to 0.058 eV between 510 and 990 K. There is also a semiconductor–metal transition at 990 K for $BiSr_{0.5}Ca_{0.5}Mn_2O_6$. The transition temperature increases with the contents of Ca. However, the activation energy decreases when Sr is substituted by Ca.

The substitution of La for Bi makes resistivity decrease too. The plot of ln ρ vs $1/T$ for $Bi_{0.5}La_{0.5}SrMn_2O_6$ is also shown in Fig. 4. There are also two transition points in the plot. Just like in $BiSrMn_2O_6$, the first point appears at 500 K. The activation energy is 0.16 eV below 500 K. It decreases to 0.046 eV between 500 and 760 K. The second transition point is not clear. It appears around 760 K. Above 760 K, the activation energy, 0.01 eV, is very low. However, unlike $BiSrMn_2O_6$, the compound still does not change to metal. This may be due to the change of energy band made by the substitution of La for Bi.

From Fig. 4, it can be seen that both the substitution of Ca for Sr and of La for Bi makes the activation energy decrease. However, the effect of substitution of La for Bi on the activation energy is more pronounced than that of the substitution of Ca for Sr. Therefore, the effect of the substitution of La for Bi on the energy band is more pro-

nounced than that of the substitution of Ca for Sr. The substitution of La for Bi even makes the metal–semiconductor transition disappear. The metal–semiconductor transition can be affected by electron densities (19). For example, in the system $Ca_{n-1}Ti_nO_{3n+1-\delta}$, transition temperatures are depressed with increasing δ (20). However, in the system $BiSr_{1-x}Ca_xMn_2O_6$, there is not obvious change of electron densities because Ca has the same valence with Sr. The major difference from Ca to Sr is that ionic radius of Ca^{2+} (0.100 nm) is smaller than that of Sr^{2+} (0.118 nm) (15). When Sr is substituted by Ca, unit cell parameters decrease. This can change the coordination state of Mn ions, which affects the excitation from $t_{2g}^4e_g^0$ to $t_{2g}^3e_g^1$. As it has been stated, the excitation from $t_{2g}^4e_g^0$ to $t_{2g}^3e_g^1$ leads to the semiconductor–metal transition in the system $BiSr_{1-x}Ca_xMn_2O_6$. Therefore, the temperature of the metal–semiconductor transition increases when Sr is substituted by Ca.

A negative magnetoresistivity effect is observed for the pellet of $Bi_{1-x}La_xSrMn_2O_6$. The magnetoresistance was examined at room temperature with an applied field of up to 1.5 T. The magnetoresistance ratios, $\Delta R_H/R_0$, were estimated using

$$\Delta R_H/R_0 = (R_H - R_0)/R_0.$$

R_0 is the resistivity without magnetic field on the samples. R_H is the resistivity of samples in magnetic field. $\Delta R_H = R_H - R_0$.

Figure 6 shows the magnetoresistance ratios versus applied magnetic field. The magnetoresistance ratio increases with H, and it is still not saturated at 15 G. When La contents increase, magnetoresistance ratios also increase. A great magnetoresistance effect was observed in the system $La_{1-x}A_xMnO_3$ (8–13), where A is a divalent metal such as Ca, Sr, or Ba. The hole doping leads to a mixed valence of Mn^{4+} and Mn^{3+}, which plays a key role in electronic transportation and ferromagnetism. Compared to $La_{1-x}A_xMnO_3$, a mixed valence of Mn^{4+} and Mn^{3+} also exists in $BiSrMn_2O_6$, and it is ferromagnetic. However, a GMR effect is not observed on $BiSrMn_2O_6$. The GMR effect occurs just when Bi is partly substituted by La. La^{3+} and Bi^{3+} have the same valence. The substitution of La for Bi makes the unit cell parameters decrease. However, the substitution of Ca for Sr also makes the unit cell parameters decrease and the GMR effect is not observed in the $BiSr_{1-x}Ca_xMn_2O_6$ system. Therefore, a decrease in unit cell parameters does not lead to a GMR effect when Bi is partly substituted by La. The remaining major different from La to Bi is that the electronegativity of La(1.08) is smaller than that of Bi(1.67) (21). The external layer electron numbers of Bi^{3+} do not reach the saturated 18 electron shell. Bi^{3+} has a stronger attraction to electrons than La^{3+} which has a 18 electron shell. This can affect energy band and electron transportation. When Bi is partly substituted by La, the electronic state of lattice is changed to an appropriate situation and leads to occurrence of GMR effect. This makes the magnetoresistance ratio increases with increasing La contents. Because of the effect of grain boundary, the MR effect of bulk is much smaller than that of film.

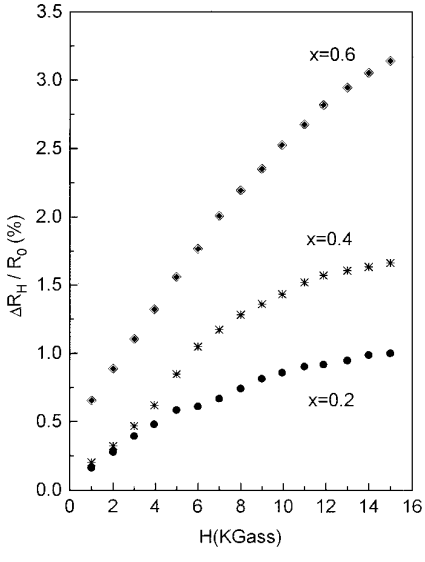

FIG. 6. Magnetoresistance ratios versus applied magnetic field of $Bi_{1-x}La_xSrMn_2O_6$.

ACKNOWLEDGMENT

This work was supported by the National Fund of China for Natural Scientific Research and the Panden Project.

REFERENCES

1. K. G. Srivatsava, *Phys. Lett.* **4,** 55 (1963).
2. J. B. Macchesney, J. F. Potter, and R. C. Sherwood, *J. Appl. Phys.* **40,** 1243 (1969).
3. C. N. R. Rao, P. Ganguly, K. K. Singh, and R. A. Mohan Ram, *J. Solid State Chem.* **72,** 13 (1988).
4. P. Ganguly and C. N. R. Rao, *J. Solid State Chem.* **53,** 193 (1984).
5. E. Pollert, S. Krupicka, and E. Kuzmicova, *J. Phys. Chem. Solids* **43**(12), 1137 (1982).
6. C. Chaumont, A. Daoudi, G. Le Flem, et P. Hagenmuller, *J. Solid State Chem.* **14,** 335 (1975).
7. V. E. Wood, A. E. Austin, E. W. Collings, and K. C. Brog, *J. Phys. Chem. Solids* **34,** 859 (1973).
8. S. Jin, T. H. Tiefel, M. McCormack, R. A. Fastnacht, R. Ramesh, and L. H. Chen, *Science* **246,** 413 (1994).
9. K. Chanara, T. Ohno, M. Kasai, and Y. Kozono, *Appl. Phys. Lett.* **63**(14), 1990 (1993).
10. R. Von Helmolt, J. Wecker, B. Holzapfel, L. Schultz, and K. Samwer, *Phys. Rev. Lett.* **71,** 2331 (1994).
11. R. Mahendiran, A. K. Raychaudhuri, A. Chainani, and D. D. Sarma, *Appl. Phys. Lett.* **66,** 233 (1995).

12. H. L. Ju, C. Kwon, Q. Li, R. L. Greene, and T. Venkateswan, *Appl. Phys. Lett.* **65,** 2108 (1994).
13. M. McCormack, S. Jin, T. Tiefel, R. M. Fleming, J. M. Phillips, and R. Ramesh, *Appl. Phys. Lett.* **64,** 3045 (1994).
14. Zeng Zuotao, Ren Yufang, and Meng Jian, *Mater. Res. Bull.* **28,** 329 (1993).
15. R. D. Shannon, *Acta Crystallogr.* **A32,** 751 (1976).
16. A. W. Sleight and G. Jones, *Acta Crystallogr.* **B31,** 2748 (1975).
17. Charles Kittel, ''Introduction to Solid State Physics,'' 6th ed. Wiley, New York, 1986.
18. C. N. R. Rao, *Ann. Rev. Phys. Chem.* **40,** 291 (1989).
19. P. Ganguly, N. Y. Vasanthacharya, C. N. R. Rao, and P. P. Edwards, *J. Solid State Chem.* **54,** 400 (1984).
20. In-Seon Kim, Mitsuruitoh, and Tetsuro Nakamura, *J. Solid State Chem.* **101,** 77 (1992).
21. Gu Qincao, Lou Shuchong, ''Handbook of Chemistry.'' Jiangsu Press of Sciences and Technologies, P.R. China, 1979.